CONTENTS

Available online at

ScienceDirect
www.sciencedirect.com

IFAC

ELSEVIER

Controllability analysis of two-phase pipeline-riser systems at riser slugging conditions

Espen Storkaas[a,1], Sigurd Skogestad[b,*]

[a]*Enhanced Operations & Production, Automation Technologies Division, ABB, Norway*
[b]*Department of Chemical Engineering, Norwegian University of Science and Technology, Trondheim, Norway*

Abstract

A PDE-based two-fluid model is used to investigate the controllability properties of a typical pipeline-riser system. Analysis of the model reveals a very interesting and challenging control problem, with the presence of both unstable poles and unstable zeros.

It is confirmed theoretically that riser slugging in pipeline-riser systems can be avoided with a simple control system that manipulate the valve at the top of the riser. The type and location of the measurement to the controller is critical. A pressure measurement located upstream of the riser (that is, at the riser base or pipeline inlet) is a good candidate for stabilizing control. On the other hand, a pressure measurements located at the top of the riser cannot be used for stabilizing control because of unstable zero dynamics. A flow measurement located at the top of the riser can be used to stabilize the process, but, because the steady state gain is close to zero, it should in practice only be used in an inner control loop in a cascade.
© 2006 Elsevier Ltd. All rights reserved.

Keywords: Process control; Stabilization; Multiphase flow; Control structure design; Petroleum industry; Anti slug control

1. Introduction

Stabilization of desired fluid flow regimes in pipelines has the potential for immense economical benefits. The opportunities for control engineers in this field are large, as control technology has only just started to make a significant impact in this area. Pipeline flow has commonly been analyzed based the on the flow regimes that "naturally" develop in the pipeline under different boundary conditions. However, with feedback control, the "natural" stability of the flow regimes can be changed to facilitate improved operation.

The best known example of (open-loop) flow regime change is probably the transition from laminar to turbulent flow in single-phase pipelines which is known to occur at a Reynolds-number of about 2300. It is well known that by carefully increasing the flow rate one may achieve laminar flow at much larger *Re*-numbers, but that in this case a small knock on the pipeline will immediately change the flow to turbulent. This indicates that the laminar flow region exists for higher *Re*-numbers, but that it is unstable. In theory, stabilization of the laminar region should be possible, and some attempts have been made in applying control to this problem (e.g. see Bewley, 2000 for a survey), but short time and length scales make practical applications difficult.

Another unstable flow phenomenon occurs in multiphase pipelines, where pressure-flow fluctuations known as slug flow can be induced both by a velocity difference between the gas and liquid phase (hydrodynamic slugging) and by the pipeline geometry (terrain induced slugging, riser slugging) (Buller, Fuchs, & Klemp, 2002). The latter slugging phenomenon occurs at a time and length scale that makes control a viable option and is the focus of this paper.

Multiphase flow may change between different flow regimes. A typical flow regime map for a pipeline-riser system is shown in Fig. 1. The flow regime map is taken from Taitel (1986), and includes some theoretical stability

---

*Corresponding author.

E-mail address: skoge@chemeng.ntnu.no (S. Skogestad).

[1]Previously with Department of Chemical Engineering, Norwegian University of Science and Technology, Norway.

conditions. It is important to notice that flow regime maps such as the one in Fig. 1, apply without control. With feedback control, these boundaries can be moved, thereby stabilizing a desirable flow regime where riser slugging "naturally" occurs.

Traditionally, undesirable slugging has been avoided in offshore oil/gas pipelines by other means than control, for example, by adding gas lift or increasing the gas lift rate, changing the operating point or making design modifications (Sarica & Tengesdal, 2000). Up until very recently, the standard method for avoiding this problem was to change the operating point by reducing the choke valve opening. However, the resulting increase in pressure results in an economic loss.

In many cases the problems with unstable flow regimes occur as the oilfields get older and the gas-to-oil ratio and water fraction increases. Since these transport systems are highly capital cost intensive, retrofitting or rebuilding is rarely an option. Thus, an effective way to stabilize the desired unstable flow regimes is clearly the best option.

The first study that applied control to this problem and by that avoided the formation of riser slugging was reported by Schmidt, Brill, and Beggs (1979). The use of feedback control to avoid severe slugging was also proposed and applied on a test rig by Hedne and Linga (1990), but this did not result in any reported implementations. More recently, there has been a renewed interest in control-based solutions (Havre, Stornes, & Stray, 2000; Hollenberg, de Wolf, & Meiring, 1995; Henriot, Courbot, Heintze, & Moyeux, 1999; Skofteland & Godhavn, 2003). These applications are either experimental or based on simulations using commercial simulators such as OLGA (Bendiksen, Malnes, Moe, & Nuland, 1991). None of the

control systems are based on a first principles dynamic model and subsequent analysis and controller design. Several industrial applications are also reported (Courbot, 1996; Havre & Dalsmo, 2002; Havre et al., 2000; Kovalev, Cruickshank, & Purvis, 2003; Skofteland & Godhavn, 2003).

In this work, a typical riser slugging case is analyzed based on a simple first-principles model, and a controllability analysis that highlight the system characteristics that are important from a control point of view is presented. This analysis gives information on sensor/actuator selection, hardware requirements and achievable performance that are critical for a successful design of a stabilizing controller for the system.

2. Riser slugging phenomenon

The cyclic behavior of riser slugging is illustrated schematically in Fig. 2. The cyclic behavior is caused by the competing effect of the compressibility of the gas upstreams of the riser and the hydrostatic head of the liquid in the riser and can be broken down into four parts. First, gravity causes the liquid to accumulate in the low point (step 1), and a prerequisite for severe slugging to occur is that the gas and liquid velocity is low enough to allow for this accumulation. The liquid blocks the gas flow, and a continuous liquid slug is formed in the riser. As long as the hydrostatic head of the liquid in the riser increases faster than the pressure drop over the riser, the slug will continue to grow (step 2).

When the pressure drop over the riser overcomes the hydrostatic head of the liquid in the slug, the slug will be pushed out of the system and the gas will start penetrating the liquid in the riser (step 3). Since this is accompanied with a pressure drop, the gas will expand and further increase the velocities in the riser. After the majority of the liquid and the gas has left the riser, the velocity of the gas is no longer high enough to pull the liquid upwards. The liquid will start flowing back down the riser (step 4) and the accumulation of liquid starts again. A more detailed description of the severe slugging phenomenon can be found in for example Taitel (1986).
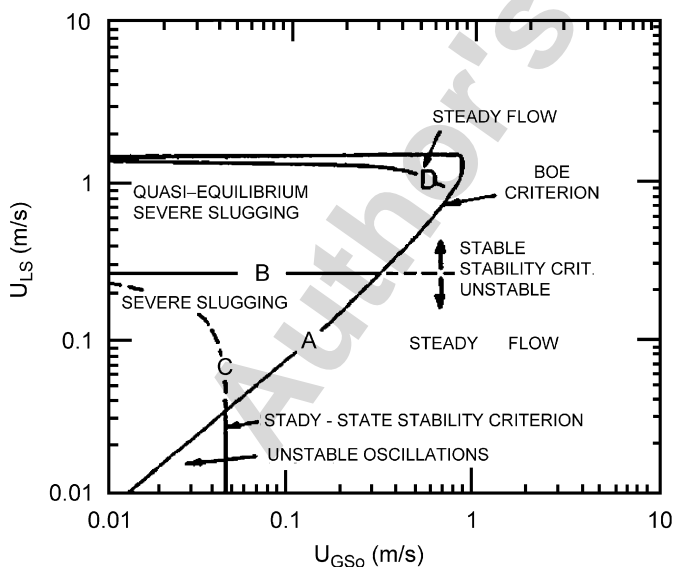

Fig. 1. Flow regime map for an experimental pipeline-riser system (Taitel, 1986). The map shows the flow regime in the pipeline as function of superficial gas and liquid velocities. Low gas and liquid velocities results in riser slugging.
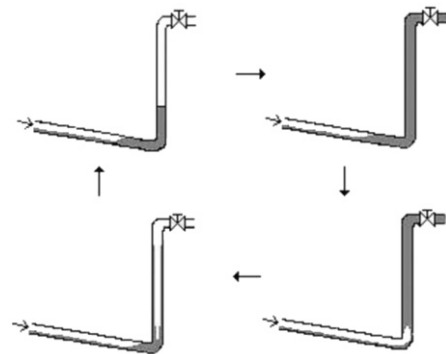

Fig. 2. Graphic illustration of a slug cycle.

It is well known that riser slugging may be avoided by choking (decreasing the valve opening Z) at the riser top. To understand why this is the case, consider a pipeline-riser system in which the flow regime initially is non-oscillatory. A positive perturbation in the liquid holdup in the riser is then introduced. Initially, the increased weight will cause the liquid to "fall down". This will result in an increased pressure drop over the riser because: (1) the upstream pipeline pressure increases both due to compression and less gas transport into the riser because of liquid blocking and (2) the pressure at the top of the riser decreases because of expansion of the gas. The increased pressure drop will increase the gas flow and push the liquid back up the riser, resulting in more liquid at the top of the riser than prior to the perturbation. Now, if the valve opening is larger than a certain critical value Z_{crit}, too much liquid will leave the system, resulting in a negative deviation in the liquid holdup that is larger than the original positive perturbation. Thus, there is an unstable situation where the oscillations grow, resulting in slug flow. For a valve opening less than the critical value Z_{crit}, the resulting decrease in the liquid holdup is smaller than the original perturbation, and the system is stable and will return to its original, non-slugging state.

3. Case description

In order to study the dominant dynamic behavior of a typical, yet simple riser slugging problem, the test case for severe slugging in OLGA (Bendiksen et al., 1991) is used. OLGA is a commercial multiphase simulator widely used in the oil industry. The nomenclature and geometry for the system are given in Fig. 3. The pipe diameter is 0.12 m. The feed into the system is nominally constant at 9 kg/s, with $W_L = 8.64$ kg/s (oil) and $W_G = 0.36$ kg/s (gas). The pressure after the choke valve (P_0) is nominally constant at 50 bar. The feed of oil and gas and the pressure P_0 are regarded as external disturbances. This leaves the choke valve opening Z as the only degree of freedom in the system.

In most real cases, the inflow is pressure dependent (W_L and W_G depends on P_I). This has some consequences on the results presented in this paper, and will be commented on when relevant. Real pipelines lie in hilly terrain which produce smaller terrain-induced slugs, but these are assumed to be included in the disturbance description introduced later.

For this case study, the critical value for the transition between a stable non-oscillatory flow regime and riser slugging is at a valve opening $Z_{crit} = 13\%$. This value was found by performing OLGA simulations for different valve openings untill a marginally stable flow regime was obtained. This is further illustrated by the OLGA simulations in Fig. 4 with valve openings of 10% (no slug), 20% (riser slugging) and 40% (riser slugging).

Simulations, such as those in Fig. 4, were used to generate the bifurcation diagram in Fig. 5, which illustrates
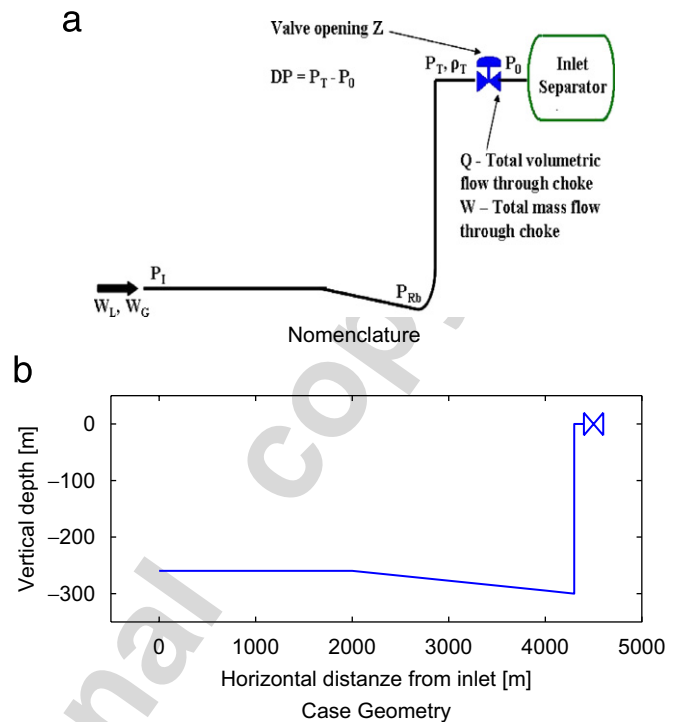
Fig. 3. (a) Nomenclature used for the pipeline riser system and (b) system geometry.
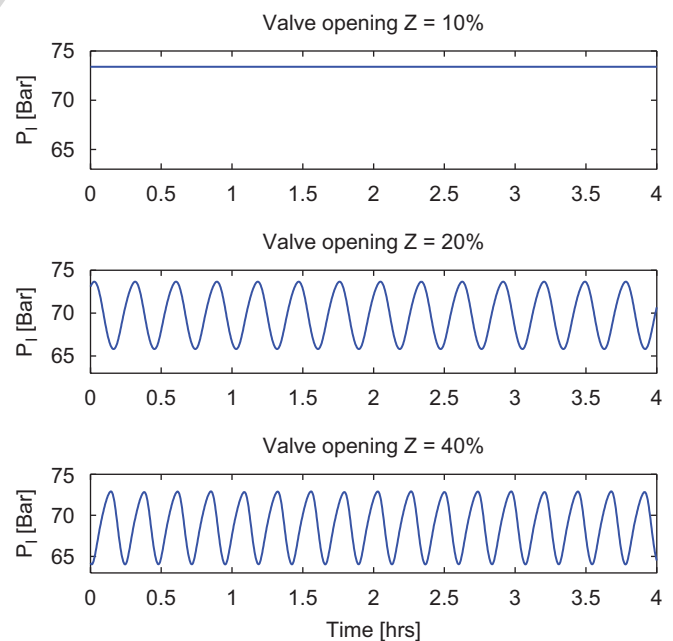
Fig. 4. OLGA simulations for valve openings of 10%, 20% and 40%.

the behavior of the system over the whole working range of the choke valve. For valve openings above 13%, the system exhibits riser slugging behavior and the two solid lines in Fig. 5 give the maximum and minimum pressure for the oscillations shown in Fig. 4. The dashed line represents the (desired) non-oscillatory flow regime, which is unstable
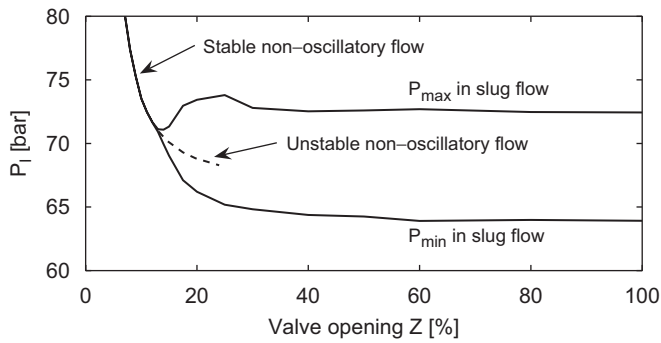
Fig. 5. Bifurcation diagram for the case study, OLGA data.

without control. Since it is unstable, it is not normally observed in OLGA simulations, but these values can be computed by initializing the OLGA model to steady-state using the OLGA steady-state processor. Thus, for choke valve openings above 13%, there are two solutions for each valve opening; one stable limit cycle and one unstable steady-state solution. For valve openings below 13%, the single solid line represents the stable non-oscillatory flow regime corresponding to the topmost simulation in Fig. 4.

4. Model description

The primary goal of this paper is to analyze the controllability properties of a system with riser slugging, and the type and complexity of the chosen model is affected by this goal. First, a model that can be linearized is needed, as the analysis methods are based on linear models. This means that the internal states of the model should be readily available and that the model should be first-order continuous (at least around the operating points). The OLGA model is not suitable as the internal states are not available. Second, some simplifying assumptions will be made that will limit the complexity of the model.

Two types of one-dimensional models are commonly used to model multiphase flow; the *drift flux model*, with mass balances for each phase and a combined momentum balance, and the *two-fluid model*, with separate mass and momentum balances for each phase. For the drift flux type model, one also needs algebraic equations relating the velocities in the different phases. More details on the modeling of slug flow can be found in for example Bendiksen, Malnes, and Nydal (1985) and Taitel and Barnea (1990).

In this work a simplified two-fluid model is used, where the conservation equations for mass and momentum for the two phases are given by the following partial differential equations (PDEs):

$$\frac{\partial}{\partial t}(\alpha_L \rho_L) + \frac{1}{A}\frac{\partial}{\partial x}(\alpha_L \rho_L u_L A) = 0, \qquad (1)$$

$$\frac{\partial}{\partial t}(\alpha_G \rho_G) + \frac{1}{A}\frac{\partial}{\partial x}(\alpha_G \rho_G u_G A) = 0, \qquad (2)$$

$$\frac{\partial}{\partial t}(\alpha_L \rho_L u_L) + \frac{1}{A}\frac{\partial}{\partial x}(\alpha_L \rho_L u_L^2 A)$$
$$= -\alpha_L \frac{\partial P}{\partial x} + \alpha_L \rho_L g_x - \frac{S_{Lw}}{A}\tau_{Lw} + \frac{S_i}{A}\tau_i, \qquad (3)$$

$$\frac{\partial}{\partial t}(\alpha_G \rho_G u_G) + \frac{1}{A}\frac{\partial}{\partial x}(\alpha_G \rho_G u_G^2 A)$$
$$= -\alpha_G \frac{\partial P}{\partial x} + \alpha_G \rho_G g_x - \frac{S_{Gw}}{A}\tau_{Gw} + \frac{S_i}{A}\tau_i. \qquad (4)$$

The notation and details regarding closure relations and model discretization are given in Appendix A. The model has four distributed dynamical states ($\alpha_L \rho_L$, $\alpha_G \rho_G$, $\alpha_L \rho_L u_L$ and $\alpha_G \rho_G u_G$), which together with the summation equation for the phase fractions $\alpha_L + \alpha_G = 1$ gives the phase fractions (α_L, α_G), gas density (ρ_G) and both velocities (u_L, u_G). The following assumptions are made:

- incompressible liquid with constant density ρ_L;
- no pressure gradient over the pipeline cross-section, implying equal pressure in both phases at a given point in the pipeline;
- no mass transfer between the phases;
- no liquid droplet field in the gas;
- isothermal conditions;
- ideal gas equation of state, corrected with a constant compressibility factor; and
- flow out of the riser can be described by the choke valve model from Sachdeva, Schmidt, Brill, and Blais (1986), which is based on a no-slip assumption for the liquid and gas and assumes incompressible liquid and adiabatic gas expansion.

Horizontal and declined flow are fundamentally different from inclined flow due to the effect of gravity. The model is based on stratified flow for the horizontal and declining pipe sections, and annular or bubbly flow for inclined pipe sections. The flow regime change from horizontal/declining pipe to inclining pipe does not introduce discontinuities, as this switch is only dependent on geometry. For more information of the flow regimes, see for example (Baker, 1954; Barnea, 1987; Mandhane, Gregory, & Aziz, 1974; Taitel & Dukler, 1976; Taitel, Barnea, & Dukler, 1980; Weisman, Duncan, Gibson, & Crawford, 1979).

It is assumed that the same algebraic relations between phase densities, velocities and friction are valid for all flow regimes, both horizontal and inclined. The expression for the wetted parameter is the only difference between the regimes. For bubble flow in inclined pipes, the wetted perimeter is computed based on an average bubble diameter. For annular flow, the wetted perimeter is that of a gas core in a body of liquid. The transition between the two flow regimes for inclined flow is modeled using a sinusoidal weighting function ($\sin(x)$, $0 \leqslant x \leqslant \pi$) and is assumed only to be a function of phase fraction ($x = f(\alpha_L)$). The model is implemented in Matlab, and is available on the internet (Storkaas, 2004).

5. Model tuning and verification

The model described above is similar, but significantly simplified, compared to the one used in OLGA. For the purpose of this work, the OLGA model is assumed to accurately describe the (imaginary) real system, and data from the OLGA simulations are used to tune the model by fitting its parameters.

The level of tuning required for any mathematical model depends on the assumptions and simplifications made. In this case, it is assumed that the liquid density is constant. In fact, the density varies weakly with pressure, and a density that is representative for the current problem is needed. The same can be said about the equation of state; the ideal gas law is used for simplicity, and some tuning on the gas molecular weight and/or compressibility factor is needed as these change throughout the system. Other important tuning parameters are the proportionality constants in the friction correlations and the average bubble diameter for bubbly flow in the riser (for determining wetted perimeter in inter-phase friction).

Still, even with all these tuning factors, obtaining a good fit to the data for all valve openings is difficult. The system is distributed, and the effect of each tuning parameter is not always clear. The focus has been to achieve a good qualitative fit to the data, as the main interest is to study the general behavior of such a system. Also, for stabilizing control, the main focus is studying the unstable stationary operating points (dashed line in Fig. 5) rather than the stable, undesired slug flow. Thus, the model is fitted mainly to the stationary (unstable) operating line, and less emphasis is put on the open-loop (uncontrolled) riser slugging behavior.

The tuning was done by manually adjusting the model parameters using the bifurcation diagrams as tuning aids. The resulting fit is illustrated in Fig. 6, where the bold lines are the reference data (OLGA) and the thin lines are computed from the simple two-fluid model. The fit for the stable non-oscillatory flow regime (at low valve openings) is excellent, especially for the risertop pressure (Fig. 6(b)), whereas there are some deviations for the slug flow regime. Since the slug flow regime is undesirable, these deviations are, as mentioned above, of less importance for control purposes.

6. Controllability analysis

The riser slugging case is interesting and challenging for control because it turns out to contain many conflicting controllability limitations. The riser slugging phenomena is oscillatory, and it is found, as expected, that the unstable (RHP) poles p_i are complex. The most serious challenge for stabilizing control (avoiding riser slugging), is that there, for some measurement alternatives, also are unstable (RHP) zeros z located close to the unstable (RHP) poles p_i. To motivate the controllability analysis, some of the
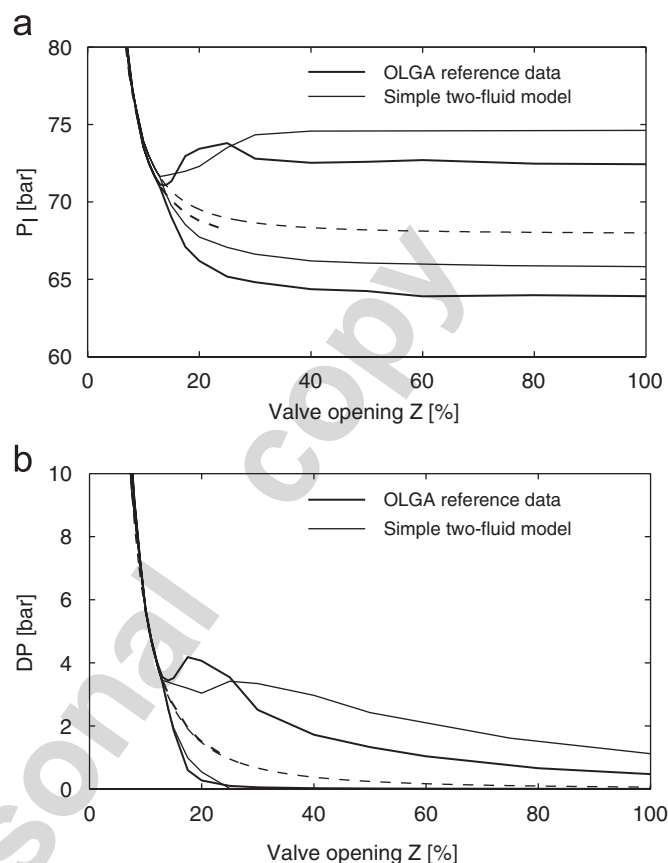

Fig. 6. Verification of tuned model for: (a) inlet pressure P_I and (b) pressure drop over choke valve DP.

controllability problems will be illustrated by simulations before some control theory is reviewed.

6.1. Introductory open-loop simulations

The main objective for anti-slug control is to stabilize the non-oscillatory flow regime using the valve position Z as a manipulated variable. In theory, for linear systems, any measurement where the instability is observable may be used (Skogestad & Postlethwaite, 1996). However, in practice input saturation (in magnitude or rate) or unstable zero dynamics (RHP-zeros) may prevent stabilization. To gain some insight into the dynamic properties, Fig. 7 shows the simulated response to a step change in Z at $t = 0$ for four alternative measurements: inlet pressure (P_I), riser base pressure (P_{Rb}), pressure drop over topside choke valve (DP) and volumetric flow out of the riser (Q). The responses are shown both for the simple two-fluid model (thin lines) and OLGA (bold lines).

The valve position prior to the step is $Z = 10\%$, and a 2% step increase is applied, so this it at a point close to instability. The simulations show that the step change induces oscillations, but because the step is made at a stable operating point, these eventually die out. The oscillations for the OLGA simulation have a period of a 25 min,
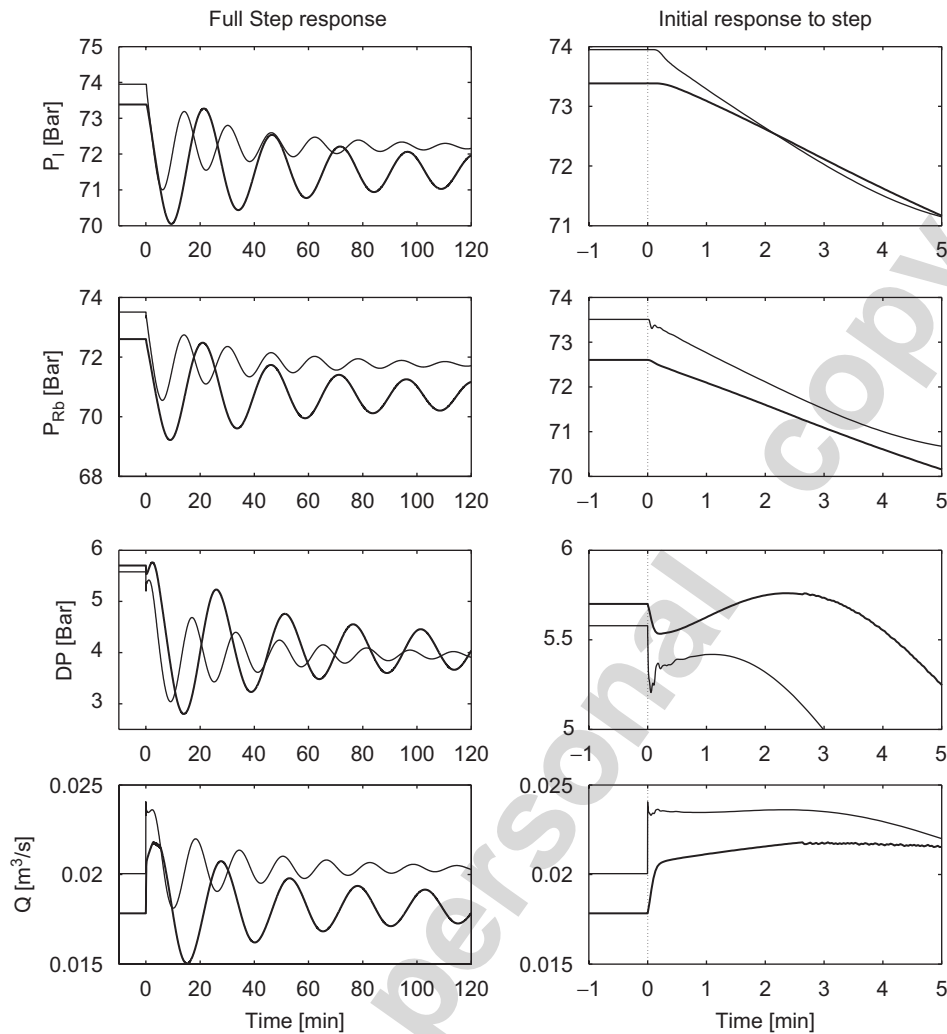
Fig. 7. Open-loop responses with the simple two-fluid model (thin lines) and OLGA (bold lines) for a step in valve opening Z.

corresponding to a frequency of $p = 2\pi/(25-60\,\text{s}) = 0.004\,\text{s}^{-1}$. The oscillations are a bit faster for the two-fluid model, with a period of about 17 min corresponding to a frequency $p = 0.006\,\text{s}^{-1}$.

For the three pressures, the main difference is for the initial response shown at the right. The P_{Rb}, there is an immediate decreasing initial response and no problems with stabilization are expected. For P_I, there is an effective delay of about 10 s, which will make stabilization a bit more difficult, but the time delay is probably not large enough to cause major problems. For DP there is also an effective delay of about 2 min with the two-fluid model and 4 min with OLGA, caused by inverse response. Finally, for the flow Q, the response is immediate, it is noted that the steady-state gain is close to zero as Q eventually returns to its original value. This means that control of Q cannot be used to affect the steady-state behavior of the system. The small steady-state gain for Q is easily explained because the inflow to the system is given, and the outflow must at steady-state equal the inflow.

The inverse responses in the time domain for the measurement $y = DP$ correspond to RHP-zeros in the transfer function model (Skogestad & Postlethwaite, 1996). Also, the shape of the inverse response, with the initial response is in the "right" direction followed by a correction in the "wrong" direction, indicate a complex pair of RHP-zeros. The transfer functions can be used to derive more exact expressions for the deteriorating effect the RHP-zeros have on control performance. Such expressions are discussed next.

6.2. Controllability analysis: Theoretical background

6.2.1. Transfer functions

Consider a process $y = G(s)u + G_d(s)d$ and a feedback controller $u = K(s)(r - y - n)$ where d represents disturbances and n the noise. The closed-loop response is

$$y = Tr + SG_d d - Tn, \tag{5}$$

where $S = (I + GK)^{-1}$ and $T = GK(I + GK)^{-1} = I - S$ are the sensitivity and complementary sensitivity function, respectively. The closed-loop input to the plant is

$$u = KS(r - G_d d - n). \tag{6}$$

In addition to the closed-loop transfer functions in (5) and (6), the transfer function SG gives the effect of input disturbances on the output y (set $G_d = G$ in (6)). The transfer functions S, T, KS and SG can also be interpreted as robustness to various kinds of uncertainty, where small magnitudes for the closed-loop transfer functions indicates good robustness properties. For example, S is the sensitivity toward inverse relative uncertainty, which is a good model of uncertainty in the pole locations (Skogestad & Postlethwaite, 1996).

Thus, by calculating the lower bounds for the closed-loop transfer functions S, T, KS, SG, KSG_d and SG_d, information can be obtained regarding both achievable performance and possible robustness problems. The bounds on the $\mathscr{H}_\infty$ norm, $\|M\|_\infty = \max_\omega |M(j\omega)|$, which is simply the peak value of the transfer function, will be considered. The bounds presented below are all independent of the controller K, and are thus a property of the process itself. The bounds are, however, dependent on a systematic and correct scaling of the process, which will be addressed after the bounds has been introduced.

6.2.2. Lower bound on S and T

The lowest achievable peaks in sensitivity and complementary functions, denoted $M_{S,min}$ and $M_{T,min}$, are closely related to the distance between the unstable poles (p_i) and zeros (z_i). For SISO systems (Skogestad & Postlethwaite, 1996) show that for any unstable (RHP) zero z:

$$\|S\|_\infty \geqslant M_{S,min} = \prod_{i=1}^{N_p} \frac{|z + \bar{p}_i|}{|z - p_i|}. \tag{7}$$

Note that the bound approaches infinity as z approaches p_i.

For systems with only one unstable zero, the bound holds with equality. Chen (2000) shows that the bound in (7) also applies to $\|T\|_\infty$, and generalizes the bound to apply for MIMO systems with any number of unstable poles and zeros:

$$M_{S,min} = M_{T,min}$$
$$= \sqrt{1 + \bar{\sigma}^2(Q_p^{-1/2} Q_{zp}^T Q_z^{-1/2})}, \tag{8}$$

where the elements of the matrices Q_z, Q_p and Q_{zp} are given by

$$[Q_z]_{ij} = \frac{y_{z,i}^H y_{z,j}}{z_i + \bar{z}_j}, \quad [Q_p]_{ij} = \frac{y_{p,i}^H y_{p,j}}{\bar{p}_i + p_j}, \quad [Q_{zp}]_{ij} = \frac{y_{z,i}^H y_{p,j}}{z_i - p_j}. \tag{9}$$

The vectors $y_{z,i}$ and $y_{p,i}$ are the (unit) output direction vectors associated with the zero z_i and pole p_i, respectively. For SISO systems, these direction vectors all equal 1.

Time delays pose additional limitations. For example, Chen (2000) shows that the bound for $\|T\|_\infty$ is increased by a factor $|e^{p\theta}|$ for a single RHP-pole.

6.2.3. Lower bound on KS

The transfer function KS from measurement noise n to plant inputs u is at low frequencies closely related to the inverse of the process transfer function G. This can be seen by rewriting $KS = G^{-1}T$ (using $GKS = T$) and recalling that with integral action, $T(0) = I$. Unstable plants requires control and a connection between KS and G^{-1} is also found in the bound (Havre & Skogestad, 1997, 2001)

$$\|KS\|_\infty \geqslant |G_s(p)^{-1}|, \tag{10}$$

where G_s is the stable version of G with the RHP-poles of G mirrored into the LHP. The bound is tight (with equality) for one real unstable pole p. For multiple and complex unstable poles p_i (Glover, 1986), gives the tight bound

$$\|KS\|_\infty \geqslant 1/\underline{\sigma}_H(\mathscr{U}(G)), \tag{11}$$

where $\underline{\sigma}_H(\mathscr{U}(G))$ is the smallest Hankel singular value of the antistable part of G.

6.2.4. Lower bound on SG and SG_d

Chen (2000) reports that for any unstable zero z in G:

$$\|SG\|_\infty \geqslant |G_{ms}(z)| \prod_{i=1}^{N_p} \frac{|z + \bar{p}_i|}{|z - p_i|}, \tag{12}$$

$$\|SG_d\|_\infty \geqslant |G_{d,ms}(z)| \prod_{i=1}^{N_p} \frac{|z + \bar{p}_i|}{|z - p_i|}, \tag{13}$$

where the subscript ms denotes the stable, minimum-phase version of the transfer function (both RHP-poles and RHP-zeros mirrored into the LHP). These bounds are only tight for one unstable zero z, but since they are valid for any RHP-zero z, they can also be applied for systems with multiple unstable zeros.

6.2.5. Lower bound on KSG_d

The stable, minimum phase part $G_{d,ms}$ of G_d can be regarded as a weight on KS. Thus, for any unstable pole p (Havre & Skogestad, 1997; Skogestad & Postlethwaite, 2005):

$$\|KSG_d\|_\infty = |G_s^{-1}(p)| \cdot |G_{d,ms}(p)|. \tag{14}$$

The bound is only tight for one real unstable pole p. For multiple and complex unstable poles p_i, the following bound is tight (Skogestad & Postlethwaite, 2005):

$$\|KSG_d\|_\infty \geqslant 1/\underline{\sigma}_H(\mathscr{U}(G_{d,ms}^{-1}G)). \tag{15}$$

6.2.6. Pole vectors

For a plant $G(s)$ with state space realization (A, B, C, D), the output pole vector $y_{p,i}$ for a pole p_i is defined by Havre and Skogestad (2003)

$$y_{p,i} = Ct_i, \tag{16}$$

where t_i is the right (normalized) eigenvector corresponding to p_i ($At_i = p_i t_i$). Havre and Skogestad (2003) finds, based on minimum input usage for stabilization, that the measurement corresponding to the largest element in the output pole vectors should be used for stabilizing control. Correspondingly, for input selection, the input that has the largest element in the input pole vector $u_{p,i} = B^H q_i$, where

q_i is the left eigenvector of A ($q_i^H A = p_i q_i^H$), should be selected. One limitation on the use of pole vectors is that the relationship between the magnitude of the input usage and the magnitude of the pole vectors elements only holds for plants with a single unstable pole p. In this case, there is a pair of complex conjugate unstable poles p_i, but it will be shown that the pole vectors still give some information about measurement selection.

6.2.7. Low frequency performance

Disturbance rejection is not strictly required for stabilizing control. However, to avoid the possible destabilizing effect of nonlinearity, the system should not "drift" too far away from its nominal operating point. To achieve low-frequency performance, the low-frequency gain must be sufficiently large. Specifically, for perfect low-frequency disturbance rejection, it is required that $|G(j\omega)| \geqslant |G_d(j\omega)|$ at frequencies $\omega > \omega_d$ where $|G_d| > 1$.

6.3. Scaling

The models are scaled as outlined in Skogestad and Postlethwaite (1996), such that all signals in the system should be less than one in magnitude. This is both to include saturation effects and to be able to compare signals of different magnitude.

The outputs are scaled with respect to the maximum allowed deviation given in Tables 1 and 2. These allowed deviations are set such that they are of equal magnitude compared to the expected variations, and should thus allow for direct comparison between the different measurement with respect to stabilizing control. Nonlinear effects cause the process gain to vary with valve opening, and in this case, the gain is smallest for large valve openings. Therefore, the input is scaled with the maximum allowed positive deviation in valve opening. For example, with a nominal valve opening of $Z = 30\%$, the input scaling is $D_u = 70\%$.

There are several different sources for uneven flow into the riser in a pipeline-riser system. First, the feed into the pipeline itself can vary, caused by upstream events (e.g changed production rate, routing of a different subset of wells into the pipeline or unstable wells). Second, hydrodynamic slugging, caused by the velocity difference between the liquid and the gas, can occur in the pipeline and give rise to uneven flow. Finally, terrain slugs, caused by accumulation of liquid in local low-points in the

Table 1
Controllability data for the operating point $Z = 17.5\%$

Measurement	Value	Scaling D_y	Smallest RHP-zero[b]	Pole vector[b]	$|G(0)|$[b]	Minimum bound on peaks[a]				
						$|S| = |T|$	$|KS|$	$|SG|$	$|KSG_d|$	$|SG_d|$
P_I [bar]	70	1	99[c]	0.36	18.9	1.0	0.03	0.0	0.06	0.0
P_{Rb} [bar]	69.5	1	1155[c]	0.37	19.0	1.0	0.03	0.0	0.06	0.0
DP [bar]	1.92	1	$0.01 \pm 0.01i$	0.21	17.6	1.6	0.04	17.1	0.08	0.95
ρ_T [kg/m³]	432	50	0.016	0.28	1.5	1.4	0.03	28.6	0.07	1.60
W [kg/s]	9	1	–[c]	0.59	0	1	0.02	0	0.06	0
Q [m³/s]	0.0208	0.002	–[c]	0.51	1.8	1	0.02	0	0.06	0

Unstable poles at $p = 0.0014 \pm 0.0085i$.
[a]Want these small.
[b]Want these large.
[c]RHP-zeros that are not important for the control problem.

Table 2
Controllability data for the operating point $Z = 30\%$

Measurement	Value	Scaling D_y	Smallest RHP-zero[b]	Pole vector[b]	$|G(0)|$[b]	Minimum bound on peaks[a]				
						$|S| = |T|$	$|KS|$	$|SG|$	$|KSG_d|$	$|SG_d|$
P_I [bar]	68.7	1	98.1[c]	0.30	3.3	1.0	0.30	0.0	0.35	0.005
P_{Rb} [bar]	68.2	1	1140[c]	0.31	3.3	1.0	0.28	0.0	0.33	0.004
DP [bar]	0.66	0.5	$0.01 \pm 0.01i$	0.17	6.1	4.3	0.62	16.8	0.97	5.5
ρ_T [kg/m³]	427	50	0.015	9.27	0.27	2.6	0.64	14.6	0.55	4.7
W [kg/s]	9	1	–[c]	0.63	0	1	0.17	0	0.32	0
Q [m³/s]	0.0211	0.002	–[c]	0.59	0.33	1	0.17	0	0.32	0.002

Unstable poles at $p = 0.0045 \pm 0.0108i$.
[a]Want these small.
[b]Want these large.
[c]RHP-zeros that are not important for the control problem.

pipeline, can create small or medium-sized slugs in the pipeline. Flow variations into the pipeline are easily represented as weighted feed disturbances. To include the effect of hydrodynamic and terrain slugging in the controllability analysis without having to include the physical effects that cause these phenomena in the model, it is assumed that the effect of hydrodynamic and terrain induced slugging can be approximated as sinusoidal feed disturbances. Thus, it is assumed that the feed disturbances W_L and W_G are frequency-dependent. The disturbance weight

$$D = 0.2 \frac{\left(\frac{2\pi}{180}s + 1\right)\left(\frac{2\pi}{160}s + 1\right)}{\left(\frac{2\pi}{90}s + 1\right)\left(\frac{2\pi}{30}s + 1\right)^2}, \tag{17}$$

will give the disturbance distribution in Fig. 8. This disturbance weight allows for a 20% variation for the stationary value of the feed for each phase, and has a peak in the frequency range 0.03–$0.2\,\mathrm{s}^{-1}$, corresponding to slug periods between 3 min and 30 s.

The downstream pressure P_0 is scaled to allowed for a frequency-independent variation of 1 bar.

6.4. Stability—poles

When the valve opening is increased, the stationary operating point moves along the single solid line in Fig. 6, through the bifurcation point at valve opening $Z_{crit} = 13\%$ and onwards along the dashed line for the unstable operating points. At the bifurcation point, there is a pair of complex poles (eigenvalues of the state matrix A of the linearized model) that cross into the right half plane, as seen from the root-locus plot in Fig. 9. This indicates that the bifurcation point is a Hopf bifurcation (Thompson & Stewart, 1986; Zakarian, 2000), which is also consistent with the shape of the bifurcation maps in Fig. 6.

Note that, as expected, the frequency of the oscillations ($p = 0.006\,\mathrm{s}^{-1}$) observed for the step change from $Z = 10$–12% in Fig. 7 correspond very closely to the imaginary parts of the poles in the Fig. 9.
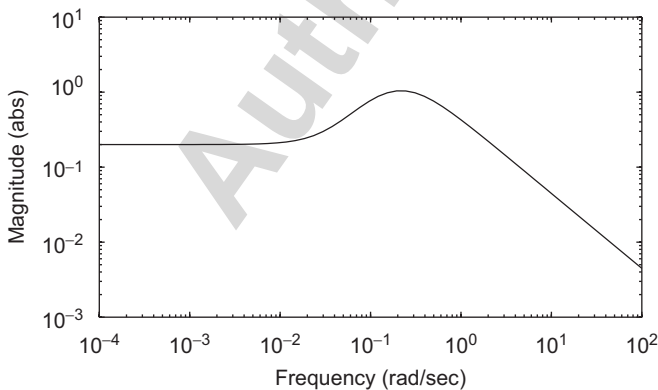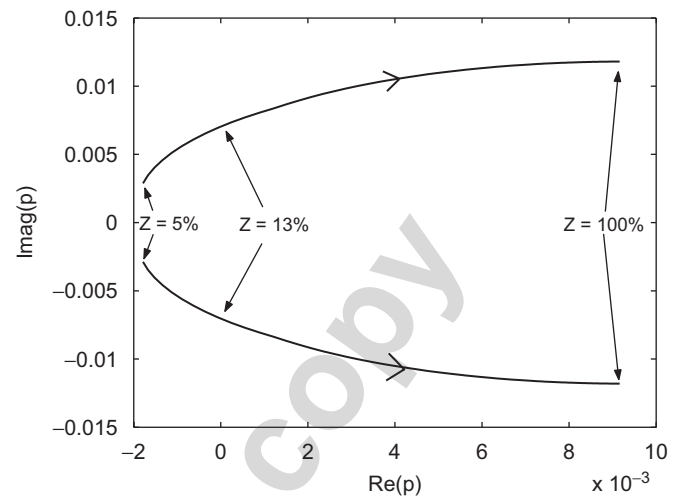

Fig. 9. Open-loop root-locus plot with valve opening Z as independent parameter. Instability occurs at for $Z \geqslant 13\%$.

6.5. Measurement evaluation

In the following sections, two different operating points are studied, one at valve opening $Z = 17.5\%$, where the instability is fairly slow, and one at valve opening $Z = 30\%$, where the instability is faster and stabilization is more difficult. The process model G and disturbance model G_d is obtained from linearizing the discretized PDE model around these two operating points.

Pressure measurements are the most reliable measurements for stabilizing these systems. The location of the pressure sensor has a significant impact on the location of the RHP-zeros and hence on the controllability of the system. In Fig. 10, the minimal achievable peak ($M_{S,min} = M_{T,min}$ in Eq. (8)) for the sensitivity functions S and T is plotted against pressure sensor location for the operating point with $Z = 30\%$. Fig. 10 show that pressure measurements located in the horizontal or declining part of the pipeline (upstream of the riser) have a peak of 1 because there are no RHP-zeros that limit performance. However, as the pressure measurement is moved up the riser toward the choke valve, the peak exceeds 4 as the fastest RHP-zero moves closer to the unstable pole, making stabilizing control more difficult.

Note that the effective time delay, which will increase as the pressure measurement is moved toward the pipeline inlet, is not included in Fig. 10. From the step responses in Fig. 7, the effective time delay to the pipeline inlet is about $10\,\mathrm{s}$, which will increase $M_{T,min}$ with a factor of about $|\mathrm{e}^{|p_i|\theta}| = \mathrm{e}^{0.011 \cdot 10} \approx 1.1$. Thus, the line for $M_{S,min} = M_{T,min}$ in Fig. 10 should slope slightly upwards toward the inlet, but the time delay is not large enough in this case to make a significant impact.

For practical reasons, the pressure sensors are usually located at the pipeline inlet (P_I) and at the choke valve (P_T). For some pipelines, there is also a pressure measurement at the riser base (P_{Rb}). Since it is assumed that the pressure P_0 behind (downstream) the choke valve

Fig. 8. Disturbance weight to allow for hydrodynamic and terrain induced slugs in the feed pipeline.
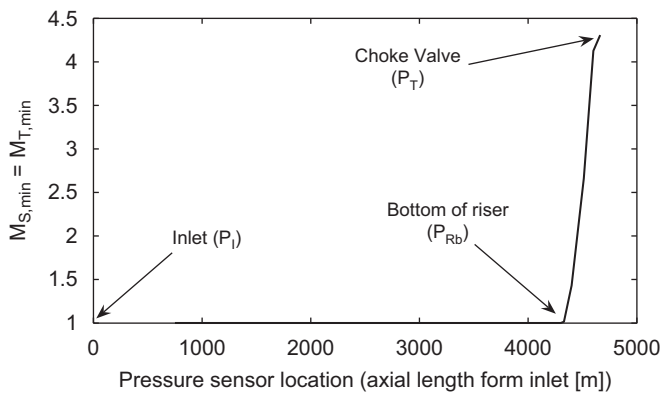
Fig. 10. Minimum peaks on $|S|$ and $|T|$ (as given by the relative distance between RHP-poles p and RHP-zeros z) as function of pressure sensor location in pipeline.

is constant, the pressure drop $(DP = P_T - P_0)$ over the choke and the pressure in front of the choke (P_T) are equivalent. In addition to these pressure measurements, the density at the top of the riser (ρ_T), the mass flow through the choke (W) and the volumetric flow through the choke (Q) is included as measurement candidates for stabilizing control.

Tables 1 and 2 summarizes the controllability results for the two operating points. The tables give the nominal value for each measurement, scaling factor, the location of the smallest unstable (RHP) zero, pole vector elements, nominal value, stationary gain as well as the lower bounds on all the closed-loop transfer functions. The following conclusions can be drawn from the tables:

- It is theoretically possible (with no model error) to stabilize the system with all the measurement candidates since the input magnitude given by $\|KS\|_\infty$ and $\|KSG_d\|_\infty$ are less than unity for all measurement candidates.
- Upstream pressure measurements $(P_I$ and $P_{Rb})$ are particularly well suited for stabilizing control with a large steady-state gain and all peaks small.
- In practice, the pressure drop over the valve (DP) and density at the top of the riser (ρ_T) should not be used for stabilizing control because of the high peaks for $|S|$ and $|T|$ (about 4), indicating robustness problems. The peak for $|SG|$ is also large (about 20). The high peaks for these transfer function are caused by RHP-zeros z close to the RHP-poles p.
- Flow measurements at the pipeline outlet $(W$ or $Q)$ can be used for stabilizing control, also in practice. However, they both suffer from a close-to zero stationary gain $(|G(0)| = 0$ and 0.33, respectively), which means that good low-frequency (steady-state) performance is not possible. Note that the mass flow W has zero stationary gain because we assume that the feed rate is constant. For real systems, the feed rate is pressure dependent, and there would be a non-zero low-frequency gain, but it would probably still be too small to allow for acceptable low-frequency performance.

- The pole vectors give the same general conclusions as the closed-loop peaks, but since the link between pole vectors and measurement selection only holds for plants with a single unstable pole, the difference between the pole vector elements for the good and the bad control variables is not very large.

6.6. Controllability analysis of flow control $(y = Q)$

From Table 2, the potential problem with flow control $(y = Q)$ is a low steady-state gain. This is confirmed in Fig. 11 the Bode magnitude plot of the linear scaled process model $G(s)$ obtained at the operating point $Z = 30\%$, together with the models $G_d(s)$ for the three disturbances. The disturbance gain for the flow disturbances are high for low frequencies and drops off sharply above about $\omega = 0.2$. Above $\omega = 0.2$, flow disturbances are effectively dampened through the pipeline. The downstream pressure disturbance P_0 does not pose a problem for control. Note that the high-frequency gain for this disturbance is unrealistic, and stems from the fact that a constant scaling over all frequencies is used.

Thus, if the volumetric flow $(y = Q)$ is chosen as the primary controlled variable, the controller will not be able to suppress low-frequency disturbances because the disturbance gain is higher that the process gain, $|G_d| > |G|$. This may cause a disturbance to drive the operation into a point where the controller no longer manages to stabilize the process. This implies that this measurement is best suited to use in an inner loop in a cascade controller, rather than for independent stabilizing control.

6.7. Controllability analysis of upstream pressure control $(y = P_I$ or $y = P_{Rb})$

From Tables 1 and 2, the upstream pressure measurements P_I and P_{Rb} both seem to be very promising candidates for control. The Bode magnitude plot of the
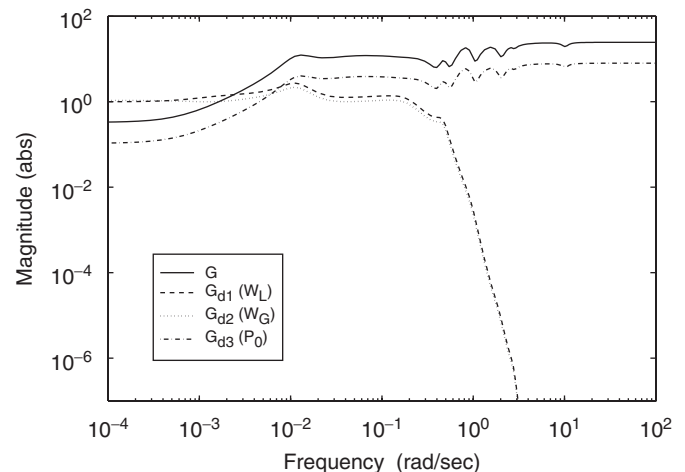

Fig. 11. Frequency dependent gain for $y = Q$ at operating point $Z = 30\%$.

linear scaled process model $G(s)$ for the inlet pressure $y = P_I$, obtained at the operating point $Z = 30\%$, is shown in Fig. 12 together with the three disturbance models. The corresponding Bode plot for the riser base pressure ($y = P_{Rb}$) is almost identical. The process gain is higher that the disturbances, $|G| > |G_d|$, for frequencies up to about $\omega = 0.15$. Above this frequency, the disturbance gain is lower than unity, and disturbance rejection is not strictly needed. However, the next section will show that the peak in the disturbance magnitude at $\omega \approx 0.2$ can, even if it is below 1, cause oscillatory flow out of the system and excessive valve movement for the stabilized system.

The analysis has so far not considered the main difference between the measurements P_I and P_{Rb}, which is the effective time delay due to pressure wave propagation in the pipeline. The simulations (both with OLGA and with the simple two-fluid model) in Section 6 showed that there are virtually no time delay through the riser to the riser base measurement P_{Rb}, whereas the pressure wave takes about 10 s to propagate back to the measurement P_I. This imposes an upper bound on the closed-loop bandwidth of the system, as the crossover frequency ω_c needs to be less than the inverse of the time delay θ, $\omega_c < 1/\theta$. On the other hand, the instability requires a bandwidth of approximately $\omega \geqslant |p|$ for complex unstable poles (Skogestad & Postlethwaite, 1996). With $|p| \approx 0.01$, this means that, for this operating point, a closed-loop crossover frequency in the range $0.015 < \omega_c < 0.1$ is needed when using $y = P_I$. For even longer pipelines than the one studied in this example, the time delay may be too high for the inlet pressure to be used for stabilizing control.

Thus, the analysis shows that the riser base pressure P_{Rb} and the inlet pressure P_{Rb} are good candidates for stabilizing control of these systems. With either of these measurements, it should be possible to design a controller that stabilize the system with little input usage, is able to effectively suppress (low-frequency) disturbances, and has good setpoint tracking properties. The main concern would

be to suppress flow disturbances in the medium-to-high frequency range (flow disturbances with $\omega \approx 0.2\,\text{s}^{-1}$, corresponding to waves and/or hydrodynamic slugging with a period of about 30 s).

6.8. Additional remarks

So far, the main topic has been single input-single output (SISO) control, but from the above discussion, the measurements have advantages in different frequency ranges. An upstream pressure measurement (P_I or P_{Rb}) has excellent low-frequency properties, while a measurement of the flow through the choke valve (Q or W) has good high-frequency properties. Combining these two measurements in a cascade controller or a similar control scheme that can utilize the benefits of both the measurement candidates would probably be a good way to approach the problem. Such a scheme has indeed already been reported by Skofteland and Godhavn (2003) and Godhavn, Mehrdad, and Fuchs (2005). However, analysis of such systems is outside the scope of this work.

It should also be mentioned that the operating point at $Z = 30\%$, used in the above analysis, is a fairly aggressive operating point with relatively fast instability and low process gain. If the same analysis were to be perform at the more conservative operating point ($Z = 17.5\%$), the controllability of the system would be significantly improved to a relatively minor cost in terms of pressure drop.

7. Simulations

Since direct design of model-based optimal controllers are complicated due to the complexity of the model, simple PI-controllers are used to illustrate and confirm the results from the controllability analysis in Section 6. The simulations use the simple two-fluid model described in Section 4. One reason for not using the OLGA model is that it is difficult with OLGA to impose the type of disturbances that is considered in this paper.

7.1. Stabilizing pressure control ($y = P_I$)

A simple feedback PI controller with controller gain $K_c = -0.3\,\text{bar}^{-1}$ and integral time $\tau_I = 500\,\text{s}$ stabilizes the system and give a crossover frequency of $\omega_c = 0.033\,\text{s}^{-1}$ for the operating point with $Z = 30\%$. The control system is illustrated in the left part of Fig. 13. However, nonlinear effects may make it difficult to stabilize the process directly at this operating point starting from initial severe slugging behavior. A possible solution to this problem is to initially stabilize the process at a less aggressive operating point and then change the pressure setpoint gradually to get to the desired operation point.

In Fig. 14, the process is started up without control with a constant valve opening of $Z = 30\%$. At $t = 30$ min, the controller is turned on with a setpoint of 70 bar and it is evident that the PI controller stabilizes the system.
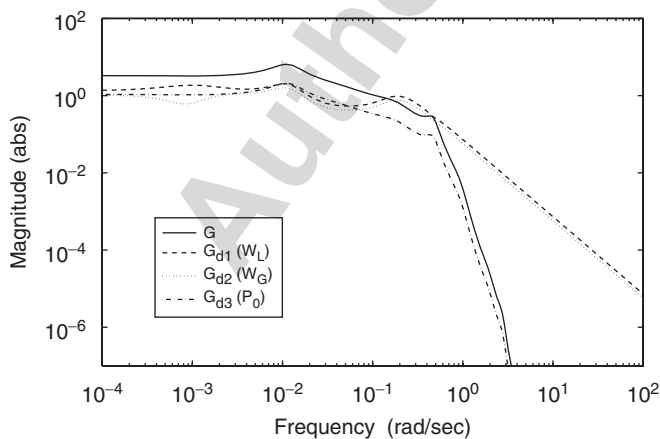

Fig. 12. Frequency dependent gain for $y = P_I$ at operating point $Z = 30\%$.
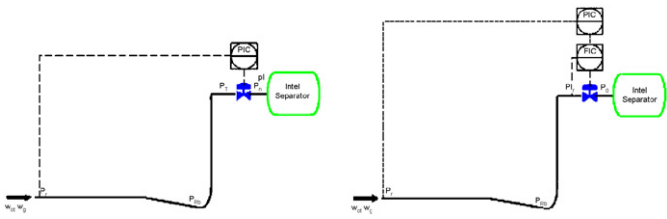
Fig. 13. Pressure control (left) and flow control (right). Dashed outer loop controller on the right hand side is a cascade controller.
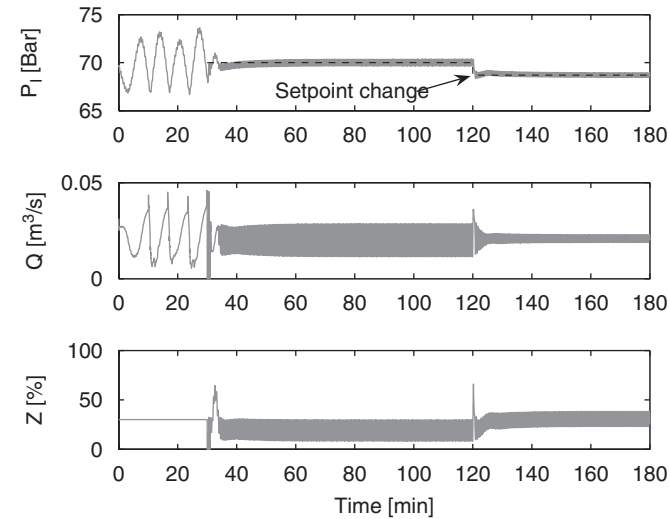

Fig. 14. Simulation of stabilizing pressure control ($y = P_I$). Controller turned on at $t = 30$ min. Setpoint change at $t = 120$ min.
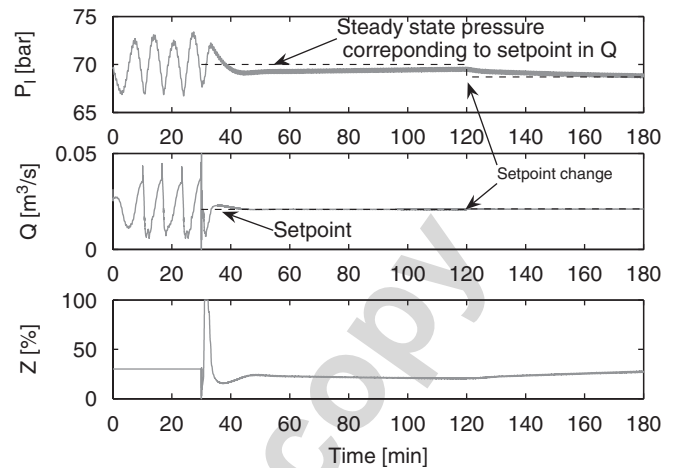

Fig. 15. Simulation of stabilizing flow control ($y = Q$). Controller turned on at $t = 30$ min. Setpoint change at $t = 120$ min.

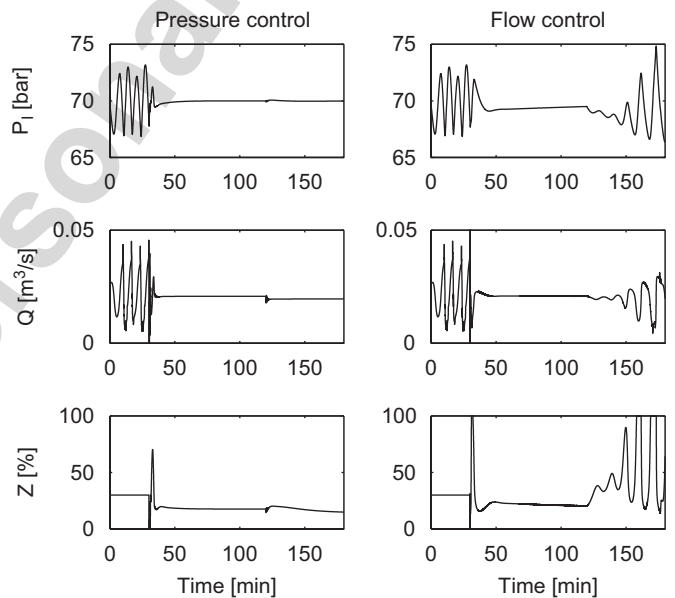

Fig. 16. Simulation of step in liquid feed at $t = 120$ min illustrating low-frequency disturbance rejection problems with flow control.

At $t = 120$ min the setpoint is changed to the desired value of 68.7 bar. Real-life hydrodynamic slugging at the inlet is represented by applying sinusoidal feed signals in counter-phase for the gas and liquid feed. The amplitude of the oscillations were $\pm 100\%$ of its nominal value, and the frequency were 0.2 rad/s. The controller manages to keep the process stable even with these large disturbances, but the valve movement and flow oscillations at the outlet are quite excessive and may be a problem.

7.2. Stabilizing flow control ($y = Q$)

To stabilize the process by controlling volumetric flow Q, a simple feedback PI controller with gain $K_c = 80 \, \text{m}^{-3}\text{s}$ and integral time $\tau_I = 500 \, \text{s}$ is used. The control system is illustrated in the right part of Fig. 13. A lag filter with two poles at $\omega = 0.5 \, \text{s}^{-1}$ is added to the controller to avoid sensitivity to noise. The crossover frequency for this system is $\omega_c = 0.28 \, \text{s}^{-1}$. As shown by the close loop simulations in Fig. 15, the setpoint for the flow is reached quickly, and the disturbance rejection is much better than the above case with pressure control. However, the low-frequency (sta-tionary) behavior of the system is very sluggish, as expected from the controllability analysis. This is illustrated by the slow return of the pressure (P_I) to its steady-state.

The poor low-frequency response is further illustrated by applying a 10% reduction in the liquid feed rate. As shown in Fig. 16, the system under flow control goes unstable because the control system cannot suppress the distur-bance. This moves the system away from its nominal operating point and into an operating region where the controller no longer can stabilize the system. The pressure control system has no problems in dealing with the step in the liquid feed rate.

The problems with flow control can at least partly be remedied by an outer loop, but the response time would depend on the input to the outer loop. An example of such a control system is shown with the dashed outer loop on the right side of Fig. 13.
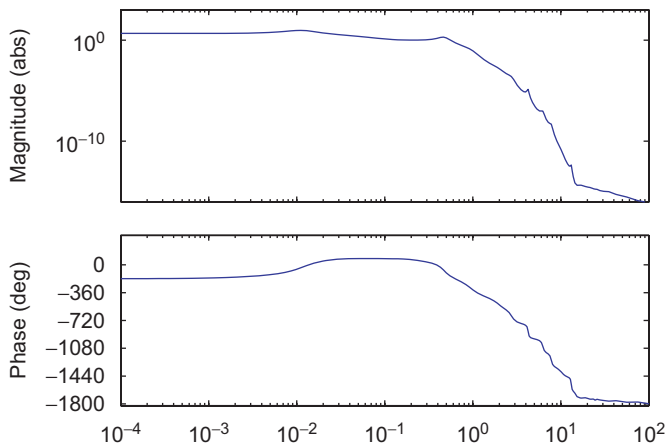
Fig. 17. Bode diagram for process model $G(s)$, $y = P_I$ at $Z = 30\%$.

8. Comments on model complexity

The PDE-model used in this paper is discretized in space to transform it into a system of ODE's that is needed for conventional controllability analysis and controller design. The drawback of this model structure is that the model order (state dimension) of the resulting system of ODE's is high (about 50 states), and the direct numerical optimization needed for design of (optimal) model based controllers gets complicated. Additionally, due to high model order, any controller based on a systematic design procedure, such as LQG control, will have a high number of states. This may be partly remedied by model reduction, but other solutions may also be conceivable.

The Bode diagram for the linear process model obtained around the operating point $Z = 30\%$ with $y = P_I$ as measurement is given in Fig. 17. Both the phase and the magnitude are relatively smooth, and resemble a significantly simpler model than the one used in this work. This leads one to suspect that the underlying mechanics of this process can be described using a greatly simplified model. This suspicion is further strengthened by physical arguments. The severe slugging is mainly a process driven by the competing effects of the pressure in the upstream (horizontal/declining) part of the pipeline and the weight of the liquid in the riser. Since both pressure and gravity are bulk quantities, it should be possible to describe the process using greatly simplified model based on bulk quantities rather than the distributed model used in this paper. Such a simplified model is presented in Storkaas (2005) and Storkaas, Skogestad, and Godhavn (2003).

9. Conclusions

In this paper, it is shown that riser slugging in pipelines can be stabilized with simple control systems, but that the type and location of the measured input to the controller is critical. Of the possible candidates studied in this work, only an upstream (inlet or riser base) pressure measure-

ment and a flow measurement at the outlet are viable candidates for stabilizing control.

Use of an upstream pressure measurement works well for stabilization, but is less suited for suppressing high-frequency flow disturbances such as small hydrodynamic slugs that might be formed in the pipeline. It might also be a problem using the inlet pressure as a primary control variable for long pipelines due to the time delay associated with pressure wave propagation.

Use of an outlet flow measurement is effective for suppressing high-frequency flow disturbances. However, the low-frequency disturbance rejection and setpoint tracking properties are poor, and this makes a stabilizing controller based on a topside flow measurement a viable option only if it is used in combination with another measurement (for example cascade or SIMO control).

The analysis of the properties of this system reveals that the underlying mechanics of the system probably can be described by a simpler model than the PDE-based model used in this work.

Appendix A. Modeling details

The PDE-based two-fluid model consist of mass balances (Eqs. (A.1) and (A.2)) and momentum balances (Eqs. (A.3) and (A.4)) for the liquid and gas phase. The balance equations combined with the summation equation for the phase fraction (Eq. (A.5)) will give the four states $\alpha_L \rho_L$, $\alpha_G \rho_G$, $\alpha_L \rho_L u_L$ and $\alpha_G \rho_G u_G$:

$$\frac{\partial}{\partial t}(\alpha_L \rho_L) + \frac{1}{A}\frac{\partial}{\partial x}(\alpha_L \rho_L u_L A) = 0, \tag{A.1}$$

$$\frac{\partial}{\partial t}(\alpha_G \rho_G) + \frac{1}{A}\frac{\partial}{\partial x}(\alpha_G \rho_G u_G A) = 0, \tag{A.2}$$

$$\frac{\partial}{\partial t}(\alpha_L \rho_L u_L) + \frac{1}{A}\frac{\partial}{\partial x}(\alpha_L \rho_L u_L^2 A)$$
$$= -\alpha_L \frac{\partial P}{\partial x} + \alpha_L \rho_L g_x - \frac{S_{Lw}}{A}\tau_{Lw} + \frac{S_i}{A}\tau_i, \tag{A.3}$$

$$\frac{\partial}{\partial t}(\alpha_G \rho_G u_G) + \frac{1}{A}\frac{\partial}{\partial x}(\alpha_G \rho_G u_G^2 A)$$
$$= -\alpha_G \frac{\partial P}{\partial x} + \alpha_G \rho_G g_x - \frac{S_{Gw}}{A}\tau_{Gw} + \frac{S_i}{A}\tau_i, \tag{A.4}$$

$$\alpha_L + \alpha_G = 1. \tag{A.5}$$

The following assumptions form the basis for the model:

- one-dimensional flow;
- constant liquid density ρ_L;

- constant pressure over a pipe cross-section, implying equal pressure in both phases;
- no mass transfer between the phases;
- no liquid droplet field in the gas;
- isothermal conditions; and
- ideal gas equation of state corrected with a compressibility factor.

The notation used for phases $k = L$ and G are given in Table A1.

Since constant liquid density ρ_L is assumed, phase fractions α_k, gas density ρ_L and phase velocities u_k can be computed directly from the states. To solve the balance equations, the shear stresses against the wall τ_{kw}, the interphase shear stress τ_i, the friction factors f_w and f_i and the wetted perimeters S_i and S_{kw} needs to be related to the state information.

The algebraic relations used for friction correlations are

$$\tau_{kw} = f_w \rho_k \frac{u_k^2}{2}, \tag{A.6}$$

$$\tau_i = f_i \rho_g \frac{(u_G - u_L)^2}{2}, \tag{A.7}$$

$$f_w = \max\left(\frac{64}{Re_k}, 0.005\left(1 + \left(\frac{2 * 10^4 \varepsilon}{D_{hk}} + \frac{10^6}{Re_k}\right)^{1/3}\right)\right), \tag{A.8}$$

$$f_i = 0.02 \frac{1 + 75\alpha_L}{4}. \tag{A.9}$$

The wetted perimeters are implicit in phase fraction, and are approximated by polynomials:

$$S_i(\text{stratified}) = (\alpha_L^2 - \alpha_L)(-4D), \tag{A.10}$$

$$S_i(\text{annular}) = \pi D \sqrt{\alpha_G}, \tag{A.11}$$

$$S_i(\text{bubble}) = \frac{\pi \alpha_G D^2}{Db}, \tag{A.12}$$

Table A1
Notation used for the two-fluid model

Symbol	Description	Unit
α_k	volume fraction	
ρ_k	density	kg/m^3
x	axial distance	m
u_k	local phase velocity	m/s
A	pipe cross-section	m^2
g_x	gravity vector in pipe direction	m/s^2
S_{kw}	wetted perim., phase k and wall	m
S_i	wetted interphase perim.	m
τ_{kw}	wall friction	Nm^2
τ_i	inter-phase friction	Nm^2
ε	wall roughness	m
D_{hk}	hydraulic diameter for phase k	m
Re_k	Reynolds number	dimensionless
Db	bubble diameter	m

$$S_{kw} = \pi \alpha_k D. \tag{A.13}$$

In order to solve the system of PDEs, they are discretized in space and the resulting set of ordinary differential equations (ODEs) are solved. A staggered grid approach is used, where the momentum equations is solved on a grid that are displaced by half a cell relative to the grid used for the mass conservation equation. This is required for numeric stability of the solution with standard ODE solvers (in this work, the built-in MatLab solver ODE23tb is used). The model is discretized using 13 grid points for the mass conservations equations and 12 grid points the momentum equations, resulting in a set of 50 ODEs. The grids points were unequally distributed, with highest density of grid points around the bottom of riser. The spatial derivatives are computed using a backward difference scheme (Patankar, 1980). Since the direction of the flow can change in this system, care has to be taken when allocating data to the ODEs. For forward flow, the data for the spatial derivatives is collected upstream the control volume, when the flow reverses, the data is collected downstream.

References

Baker, D. (1954). Simultaneous flow of oil and gas. *Oil and Gas Journal, 53,* 183–195.

Barnea, D. (1987). A unified model for predicting flow pattern transitions for the whole range of pipe inclinations. *International Journal of Multiphase Flow, 13,* 1–12.

Bendiksen, K., Malnes, D., & Nydal, O. J. (1985). On the modeling of slug flow. *Chemical Engineering Science, 40,* 59–75.

Bendiksen, K. H., Malnes, D., Moe, R., & Nuland, S. (1991). The dynamic two-fluid model OLGA: Theory and application. *SPE production engineering* (pp. 171–180).

Bewley, T. R. (2000). Flow control: New challenges for a new renaissance. *Progress in Aerospace Sciences, 37,* 21–58.

Buller, A. T., Fuchs, P., & Klemp, S. (2002). Flow assurance. *Statoil's research & technology memoir No. 1,* Available on request from authors.

Chen, J. (2000). Logarithmic integrals, interpolation bounds and performance limitations in MIMO feedback systems. *IEEE Transactions on Automatic Control, AC-45*(6), 1098–1115.

Courbot, A. (1996). Prevention of severe slugging in the Dunbar 16″ multiphase pipeline. *Offshore technology conference,* May 6–9, Houston, TX.

Glover, K. (1986). Robust stabilization of linear multivariable systems: relations to approximation. *International Journal of Control, 43*(3), 741–766.

Godhavn, J.-M., Mehrdad, P. F., & Fuchs, P. H. (2005). New slug control strategies, tuning rules and experimental results. *Journal of Process Control, 15,* 547–577.

Havre, K., & Dalsmo, M. (2002). Active feedback control as a solution to severe slugging. *SPE production and facilities* (pp. 138–148), SPE 79252.

Havre, K., & Skogestad, S. (1997). Limitations imposed by RHP zeros/poles in multivariable systems. In: *Proceedings of the European control conference,* Brussels, Number Tu-A H1.

Havre, K., & Skogestad, S. (2001). Achievable performance of multivariable systems with unstable zeros and poles. *International Journal of Control, 48,* 1131–1139.

Havre, K., & Skogestad, S. (2003). Selection of variables for stabilizing control using pole vectors. *IEEE Transaction on Automatic Control, 74*(8), 1393–1398.

Havre, K., Stornes, K. O., & Stray, H. (2000). Taming slug flow in pipelines. *ABB Review*, 4, 55–63.

Hedne, P., & Linga, H. (1990). Suppression of terrain slugging with automatic and manual riser choking. *Advances in Gas–Liquid Flows* (pp. 453–469).

Henriot, V., Courbot, A., Heintze, E., & Moyeux, L. (1999). Simulation of process to control severe slugging: Application to the Dunbar pipeline. *SPE annual conference and exhibition*, Houston, TX, SPE 56461.

Hollenberg, J. F., de Wolf, S., Meiring, & W. J. (1995). A method to supress severe slugging in flow line riser systems. *Proceedings of the seventh international conference on multiphase technology conference*.

Kovalev, K., Cruickshank, A., & Purvis, J. (2003). The slug suppression system in operation. *Offshore Europe 2003*, Aberdeen, UK, SPE 84947.

Mandhane, J. M., Gregory, G. A., & Aziz, K. (1974). A flow pattern map for gas-liquid flow in horizontal pipes. *International Journal of Multiphase Flow*, 1, 537–553.

Patankar, S.V. (1980). *Numerical heat transfer and fluid flow*. Series in computational methods in mechanics and thermal sciences. Washington, DC: Hemisphere Publishing Company.

Sachdeva, R., Schmidt, Z., Brill, J. P., & Blais, R. M. (1986). *Two phase flow through chokes*, SPE 15657.

Sarica, C., & Tengesdal, J. Ø. (2000). A new technique to eliminating severe slugging in pipeline/riser systems. *SPE annual technical conference and exhibition*, Dallas, TX, SPE 63185.

Schmidt, Z., Brill, J. P., & Beggs, H. D. (1979). Choking can eliminate severe slugging. *Oil and Gas Journal*, 230–238.

Skofteland, G., & Godhavn, J.-M. (2003). Suppression of slugs in multiphase flow lines by active use of topside choke—field experience and experimental results. In: *Proceedings of multiphase '03*, San Remo, Italy, 11–13 June 2003.

Skogestad, S., & Postlethwaite, I. (1996). *Multivariable feedback control*. New York: Wiley.

Skogestad, S., & Postlethwaite, I. (2005). *Multivariable feedback control* (2nd ed.). New York: Wiley.

Storkaas, E. (2004). Matlab source code for nonlinear PDE model. Available at the homepage of Sigurd Skogestad: ⟨www.nt.ntnu.no/users/skoge/software/⟩.

Storkaas, E. (2005). *Stabilizing control and controllability*: Control solutions to avoid slug flow in pipeline-riser systems. Ph.D. thesis, Norwegian University of Science and Technology.

Storkaas, E., Skogestad, S., & Godhavn, J.-M. (2003). A low-dimensional model of severe slugging for controller design and analysis. In: *Proceedings of multiphase '03*, San Remo, Italy, 11–13 June 2003.

Taitel, Y. (1986). Stability of severe slugging. *International Journal of Multiphase Flow*, 12(2), 203–217.

Taitel, Y., & Barnea, D. (1990). Two phase slug flow. *Advances in Heat Transfer*, 20, 71–103.

Taitel, Y., Barnea, D., & Dukler, A. E. (1980). Modeling flow pattern transitions for steady upward gas–liquid flow in vertical tubes. *AIChE Journal*, 26, 345–354.

Taitel, Y., & Dukler, A. E. (1976). A model for predicting flow regime transitions in horizontal and near horizontal gas–liquid flow. *AIChE Journal*, 22, 47–55.

Thompson, J. M. T., & Stewart, H. B. (1986). *Nonlinear dynamics and chaos*. New York: Wiley.

Weisman, J., Duncan, D., Gibson, J., & Crawford, T. (1979). Effect of fluid properties and pipe diameter on two-phase flow patterns in horizontal lines. *International Journal of Multiphase Flow*, 5, 437–460.

Zakarian, E. (2000). Analysis of two-phase flow instabilities in pipe-riser systems. In: *Proceedings of the ASME pressure vessels and piping conference*, Seattle.